DOI: 10.1002/zaac.201300463

Synthesis, Characterization, and Catalytic Activity of Iron(II) and Nickel(II) Complexes Containing the Rigid Pentadentate Ligand PY_5Me_2

Jing Xiang,*[a] Hao Li,[a] and Jia-Shou Wu*[b]

Keywords: PY_5Me_2; Iron; Catalytic activity; C–H bond activation

Abstract. The reactions of PY_5Me_2 with hydrated metal perchlorate salts $[M^{II}(ClO_4)_2]$ in CH_3CN afforded two isostructural compounds $[M^{II}(PY_5Me_2)(CH_3CN)](ClO_4)_2$ in high yields [*M* = Fe (**1**), Ni (**2**)]. The crystal structure of **2** was determined by X-ray crystallography. The catalytic activities of **1** and **2** towards the alcohol oxidation and C–H bond activation of organic substrates were studied. Initial experiments revealed that **1** was an active catalyst for the oxidative dehydrogenation and C–H bond activation of various substrates, whereas **2** was not. A Fe^{III} species $[Fe^{III}(PY_5Me_2)(OH)]^{2+}$ was proposed as the active species for the catalytic reactions.

Introduction

The coordination chemistry of the semirigid pentadentate polypyridyl ligands PY_5R_2, (where *R* = H, Me, OH, Me) (Figure 1) has attracted wide attention.[1] These ligands typically coordinate central metal atoms by one axial and four equatorial pyridine, imposing a square-pyramidal coordination arrangement, although other coordination modes have also been reported.[2,3] Moreover, they are able to reinforce an octahedral environment and restrict ligand substitution to a single coordination site.[4] These properties are particularly important in controlling the reactivity of kinetically labile first row metals. A number of transition metal complexes (Mn, Fe, Co, Ni, Cu, and Zn) bearing these ligands have been reported and applied in a wide range of areas including single-molecule magnets,[5–9] and electrocatalytic water reduction.[10,11] The pyridine subunits of PY_5R_2 provide a neutral five-coordinate metal binding cavity. Its complexation with divalent metal results usually in a stronger Lewis acidity on the central metal atoms. Several iron PY_5R_2 complexes have been reported to mimic the iron active site in lipoxygenases (Los).[12,13] These iron complexes were found to activate 1,4-pentadiene subunit-containing fatty acids and also related model substrates into alkyl peroxides.[14,15] However, the catalytic activity of metal complexes bearing PY_5R_2 for functional transformations of organic substrates has been seldom studied, although many similar iron complexes of polypodal ligands have been used as oxidation catalysts.[16]

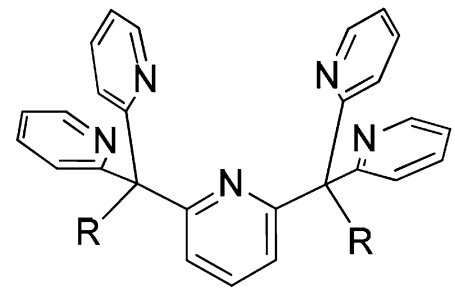

Figure 1. Structure of PY_5R_2.

Herein, we report the synthesis of nickel and iron complexes bearing the ligand 2,6-bis[1,1-bis(2-pyridyl)ethyl]pyridine (PY_5Me_2) and their catalytic oxidative dehydrogenation of various alcohols, phenol, hydroquinone, as well as the C–H bond activation of styrene and cyclohexane using H_2O_2 as the terminal oxidant.

Results and Discussion

The reactions of equimolar amounts of ligand PY_5Me_2 and hydrated Fe^{II} and Ni^{II} perchlorate salts in CH_3CN afforded two isostructural compounds $[M^{II}(PY_5Me_2)(CH_3CN)](ClO_4)_2$ [*M* = Fe (**1**); Ni (**2**)].[8] Both complexes are stable to O_2 and moisture and are isolated as microcrystalline solids at high yields. IR spectra of **1** and **2** show weak stretching bands at 2007 and 2018 cm^{-1}, respectively, which are assigned to ν(C≡N) stretches of the coordinated CH_3CN. The strong stretching bands at around 1110 cm^{-1} are assigned to ν(Cl–O) stretch of ClO_4^-. The cyclic voltammogram (CV) (Figure 2) of **1** in CH_3CN shows a quasi-reversible couple at $E_{1/2}$ = 0.75 V (ΔE_p = 71 mV) and an irreversible couple at E_{pa} = –2.09 V vs. $FeCp_2^{+/0}$ in the range of –2.5 to 1.7 V at a scan rate of 100 $mV \cdot s^{-1}$. These couples are assigned to $Fe^{III/II}$ and $Fe^{II/I}$

* Dr. J. Xiang
Fax: +86-716-8060650
E-Mail: xiangjing35991@sohu.com
* Dr. J.-S. Wu
E-Mail: jsw79@tzc.edu.cn
[a] College of Chemistry and Environmental Engineering
Yangtze University
Jingzhou 434020, HuBei, P. R. China
[b] School of Pharmaceutical and Chemical Engineering
Taizhou University
Taizhou 317000, P. R. China

Supporting information for this article is available on the WWW under **http://dx.doi.org/10.1002/zaac.201300463** or from the author.

Zeitschrift für anorganische und allgemeine Chemie ZAAC Journal of Inorganic and General Chemistry

couples respectively, as their potentials are comparable with those in other Fe^{II} compounds bearing these ligands.[2] Ligand centered oxidation and reduction occurs at potentials of > +1.0 V and < –2.3 V vs. $FeCp_2^{+/0}$, respectively, as reported in a previous study.[2] Under similar conditions, CV of **2** shows a quasi-reversible wave at $E_{1/2}$ = 1.36 V (ΔE_p = 80 mV) and a reversible wave at $E_{1/2}$ = –1.57 V (ΔE_p = 60 mV), which are tentatively assigned to $Ni^{III/II}$ and $Ni^{II/I}$ couples, respectively (Figure 2). ESI/MS of **1** in CH_3CN (+ve mode) shows two predominant peaks at *m*/*z* 249.6 and 598.2, which are assigned to the parent cation $[M]^{2+}$ and $[M + ClO_4]^+$ respectively (Figure S1, Supporting Information). ESI/MS of **2** in CH_3CN (+ve mode) shows the peaks of the corresponding cations at *m*/*z* 250.8 and 600.4, respectively (Figure S2).

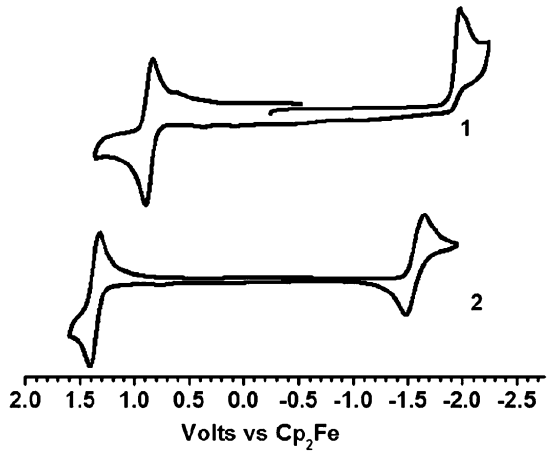

Figure 2. CVs. of **1** and **2** in 0.1 M $[NnBu_4]PF_6$ in CH_3CN. Scan rate = 100 mV s^{-1}.

The crystals of **2** suitable for X-ray crystallography were obtained by slow diffusion of diethyl ether into a CH_3CN solution of **2**. The structure of the cation is shown in Figure 3. **2** crystallizes in the triclinic $P\bar{1}$ space group. In each asymmetric unit, there is one cation and two ClO_4^-. The divalent nickel atom is ligated in a six-coordinate octahedral arrangement by the five nitrogen donors of PY_5Me_2 and an exogenous CH_3CN. The nitrogen atoms on the four terminal pyridines (N2–5) defines the equatorial plane, and the axial positions are occupied by the remaining pyridine nitrogen (N6) and an exogenous CH_3CN (N1). The Ni–N(pyridine) bond lengths are in the narrow range of 2.047(2)–2.114(2) Å. The *cis* N(pyridine)–Ni–N(pyridine) bond angles are in range of 81.87(9)–99.42(8)° and the *trans* N(pyridine)–Ni–N(CH_3CN) bond angles are in the range of 175.08(8)–177.27(8)°. These bond parameters are comparable with those in related nickel compounds[17] (Table S1, Supporting Information). The metal ion is slightly (ca. 0.07 Å) displaced from the equatorial plane toward the CH_3CN unit.

The catalytic activities of **1** and **2** towards the alcohol oxidation and C–H bond activation of various substrates were studied. Initial experiments revealed that complex **1** catalyzes the oxidative dehydrogenation of cyclohexanol, while complex **2** is not an active catalyst. Table S2 (Supporting Information) shows the results of cyclohexanol oxidation on **1** in different

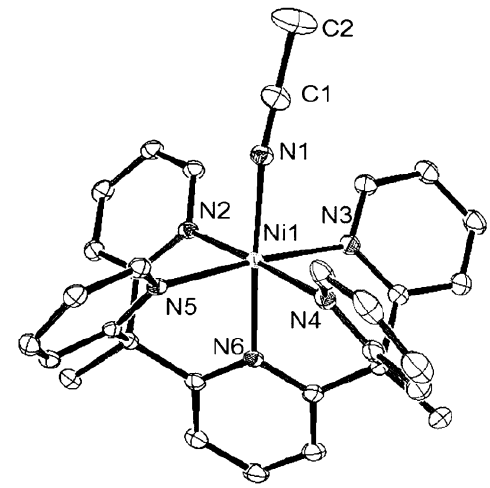

Figure 3. The ORTEP drawing of cationic structure in **2** (thermal ellipsoids are drawn at 30% probability and hydrogen atoms are omitted for clarity).

solvents using H_2O_2 as the oxidant at room temperature. In protic solvents, such as *tert*-butanol, water and trifluoroacetic acid, only small amount of ketone product were obtained (GC-FID). A better result was obtained in acetonitrile, where cyclohexanone was formed in 14% yield after 20 h. Acetone was proved to be the solvent of choice. With 1 mol equiv. H_2O_2, cyclohexanone was obtained in 20% yield after 20 h at 25 °C in an argon atmosphere in acetone solution containing 0.003 mmol **1** at a substrate/catalyst (S/C) ratio of 100 (Table S2, entry 5). With 5 mol equiv. of H_2O_2, the yield of cyclohexanone was further improved (42%) (Table S2, entry 6). The investigation was also extended to other alcohols (Table 1). Cyclopentanol and cyclohexanol were oxidized to corresponding ketone (43% yield) at room temperature (Table 1, entries 1 and 2). Benzyl alcohols could also be oxidized. When 1-phenylethanol was used, acetophenone was formed in a moderate yield of 49% (Table 1, entry 3). With more reactive and less steric benzyl alcohol, benzaldehyde was obtained selectively in 52% yield within 3 h (Table 1, entry 4). For the oxidation of aliphatic acyclic alcohol, poor yield was obtained for *n*-heptanol (14%), while a relatively better result (33%) was achieved with the more sterically hindered 2-heptanol (Table 1, entries 6 and 7). Surprisingly, *n*-butanol was not oxidized (Table 1, entry 5). Hydroquinone was also oxidized to benzoquinone (71%) with **1** as catalyst after 4 h, whereas phenol exhibited no reaction under similar conditions (Table 2, entries 1 and 2).

The oxidation of cyclohexane via C–H bond activation with **1** was also investigated and the two products, cyclohexanol and cyclohexanone, were detected at 14% and 11% yield, respectively (Table 2, entry 3), whereas the oxidation of styrene in acetone and acetonitrile gave benzaldehyde in 18% and 9% yield (Table 2, entries 4 and 5).

Stacket et al. has investigated the reaction of $[Fe(PY_5)(MeCN)](OTf)_2$ [PY = 2,6-bis(bis(2-pyridyl)methoxymethane) pyridine] with excessive H_2O_2 in methanol at 298 K, where a thermally unstable blue species that was proposed to be a low

Table 1. Oxidation of various alcohols by H_2O_2 catalyzed by $[Fe(py_5Me_2)(H_2O)](ClO_4)_2$ in acetone [a].

Entry	Substrate	Time /h	Product	Yield /%[b]
1		20		45
2		20		43
3		20		49
4		3		52
5		20	N. R.	N. R.
6	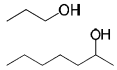	20	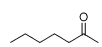	33
7	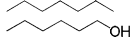	20	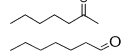	14

a) Reaction conditions: [substrate] = 3 mmol; $[H_2O_2]$ = 0.3 mmol; $[Fe(py_5Me_2)(CH_3CN)](ClO_4)_2]$ = 0.003 mmol; total solution, 3 mL. The mixture was stirred at room temperature. b) Yield of product is based on oxidant.

Table 2. Oxidation of phenol, hydroquinone, styrene, and cyclohexane by H_2O_2 catalyzed by $[Fe(py_5Me_2)(H_2O)](ClO_4)_2$ in acetone [a].

Entry	Substrate	Time /h	Product	Yield /%[b]
1		20	N. R.	N. R.
2		4		71
3		20	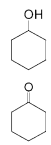	14 11
4[c]		20		18
5[d]		20		9

a) Reaction conditions: [substrate] = 3 mmol; $[H_2O_2]$ = 0.3 mmol; $[Fe(py_5Me_2)(CH_3CN)](ClO_4)_2]$ = 0.003 mmol; total solution, 3 mL. The mixture was stirred at room temperature. b) Yield of product is based on oxidant. c) Reaction conditions: [substrate] = 0.3 mmol; $[H_2O_2]$ = 0.3 mmol; $[Fe(py_5Me_2)(CH_3CN)](ClO_4)_2]$ = 0.003 mmol; in 3 mL acetone. d) Reaction conditions: [substrate] = 3 mmol; $[H_2O_2]$ = 0.3 mmol; $[Fe(py_5Me_2)(CH_3CN)](ClO_4)_2]$ = 0.003 mmol; in 3 mL acetonitrile.

spin hydroperoxide-bound ferric species, $[Fe^{III}(PY_5)(OOH)](OTf)_2$, was generated.[15] To identify the active species in our system, the ESI/MS of **1** and **2** in the presence of excess H_2O_2 was carried out in acetone. As shown in Figure 4, a strong peak at *m/z* 249.6 assigned to the $[Fe(PY_5Me_2)]^{2+}$ cation was initially observed. After the addition of 100 equiv. H_2O_2, the light yellow solution turn green immediately and the peak at *m/z* 249.6 nearly disappeared, while a predominant peak at *m/z* 258.2 tentatively assigned to the species $[Fe^{III}(PY_5Me_2)(OH)]^{2+}$ was observed. However, under the same conditions, the ESI/MS of **2** remained unchanged after addition of H_2O_2, suggesting that the oxidation of $[Ni^{II}(PY_5Me_2)]^{2+}$ into the corresponding $[Ni^{III}(PY_5Me_2)(OH)]^{2+}$ species did not occur. This suggests **2** is not an active catalyst when H_2O_2 is used as the oxidant. The oxidation of **1** to $[Fe^{III}(PY_5Me_2)(OH)]^{2+}$ with H_2O_2 is further supported by the more negative $Fe^{III/II}$ couple ($E_{1/2}$ = 0.76 V), whereas the $Ni^{III/II}$ couple in **2** occurs at much more positive potential ($E_{1/2}$ = 1.36 V). Attempts to isolate the $[Fe^{III}(PY_5Me_2)(OH)]^{2+}$ species were unsuccessful. On basis of the above results, $[Fe^{III}(PY_5Me_2)(OH)]^{2+}$ was proposed to be the active catalyst formed from the oxidation of $[Fe^{II}(PY_5Me_2)]^{2+}$ by H_2O_2 (Scheme 1). As formation of $[Fe^{III}(PY_5Me_2)(OH)]^{2+}$ in the reaction of $[Fe^{II}(PY_5Me_2)]^{2+}$ and hydrogen peroxide would also imply the generation of hydroxyl radicals, which in turn may also act as the oxidant. In order to exclude this possibility, the radical inhibitors such as CCl_3Br or coumarin was added in the reaction system; however, these reagents do not exhibit significant influence on the catalytic effect. Thus, we proposed that $[Fe^{III}(PY_5Me_2)(OH)]^{2+}$, herein, functions as the only catalyst for the present alcohol oxidation. In fact, the structurally related methoxy species $[Fe^{III}(PY_5Me_2)(OMe)]^{2+}$ was also found to activate C–H bonds of certain organic substrates.[14,15] It is believed that $[Fe^{III}(PY_5Me_2)(OH)]^{2+}$, rather than $[Fe^{III}(PY_5Me_2)(OOH)]^{2+}$, may be responsible for the oxidative dehydrogenation and C–H bond activation in this study.

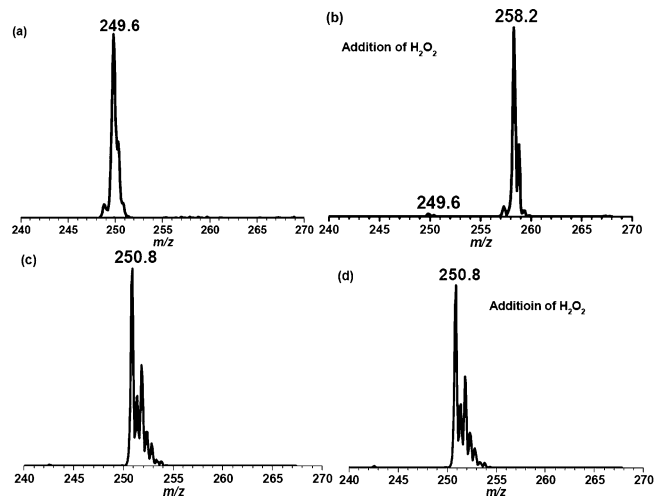

Figure 4. (a) and (b): ESI-MS of **1** in acetone (+ ve mode) before and after addition of H_2O_2; (c) and (d): ESI-MS of **2** in acetone (+ ve mode) before and after addition of H_2O_2.

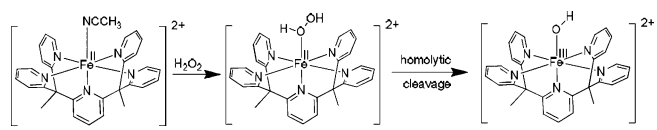

Scheme 1. The proposed active species from the reaction of **1** with H_2O_2.

Conclusions

We found that the Fe^{II} complex bearing the semi-rigid ligand PY_5Me_2 catalyzes the oxidation of various alcohols and even alkanes by H_2O_2 under mild conditions. The in situ generated $[Fe^{III}(PY_5Me_2)(OH)]^+$ was proposed to be the active species involved. No encouraging results could be obtained with the analogous Ni^{II} complex, possibly as a result of the more positive $Ni^{III/II}$ couple, which discourages the formation of the corresponding Ni^{III}–OH species. To our best knowledge, this is the first study, which demonstrates the catalytic activity of iron complexes bearing PY_5Me_2 ligand towards the functional transformations of organic substrates. It is well known that high-valent Ru complexes are usually more stable than their Fe analogues and Ru-oxo species oxidizes alcohols rapidly via a two-electron hydride abstraction process.[18,19] Thus, we will try to synthesize the ruthenium compound bearing PY_5Me_2 ligand and investigate their catalytic activity towards C–H bond activation of various substrates and develop more functional transformations in organic synthesis.

Experimental Section

The ligand 2,6-bis(1,1-bis(2-pyridyl)ethyl)pyridine (PY_5Me_2) was synthesized by a reported procedure.[20] $[n\mathrm{Bu_4N}]PF_6$ (Aldrich) used for cyclic voltammetry was recrystallized three times from boiling ethanol and dried in a vacuum at 120 °C for 24 h. Acetonitrile (Aldrich) was distilled over calcium hydride. All other chemicals were of reagent grade and used without further purification. All manipulations were performed with no precaution to exclude air or moisture unless otherwise stated.

Physical Measurements: IR spectra were obtained as KBr discs with a Nicolet 360 FTIR spectrophotometer. Elemental analysis was performed with an Elementar Vario EL Analyzer. Electrospray ionization mass spectrometry (ESI-MS) was performed with a PE-SCIEX API 365 triple quadruple mass spectrometer. Cyclic voltammetry (CV) was performed with a PAR model 273 potentiostat. Cyclic voltammetry was performed in acetonitrile containing 0.1 M $[n\mathrm{Bu_4N}]PF_6$ as the supporting electrode at room temperature. An $Ag/AgNO_3$ (0.1 M in CH_3CN) electrode was used as reference electrode and the working electrode was a glassy carbon electrode (CH Instruments, Inc.) with a platinum-wire auxiliary electrode. Ferrocenium/ferrocene ($FeCp_2^{+/0}$) was used as the internal reference. All solutions for electrochemical studies were degassed with pre-purified argon gas prior to measurements. Gas chromatographic analyses were performed with a HP5890 GC/FID equipped with HP-5MS (30 m × 0.25 mm i.d.) or a DB-FFAP (30 m × 0.25 mm i.d.) column. GC/MS measurements were carried out on a HP6890 gas chromatograph interfaced to a HP 5795 mass selective detector.

X-ray Crystallography: Measurement was collected with an Oxford CCD diffractometer using graphite-monochromated Mo-K_α radiation (λ = 0.71073 Å) for **1**. Details of the intensity data collection and crystal data are given in Table S3 (Supporting Information). Absorption corrections were done by the multiscan method. The structure was resolved by the heavy-atom Patterson method or direct methods and refined by full-matrix least-squares using SHELX-97 and expanded using Fourier techniques.[21,22] All non-hydrogen atoms were refined anisotropically. Hydrogen atoms were generated by the program SHELXL-97. The positions of hydrogen atoms were calculated on the basis of riding mode with thermal parameters equal to 1.2 times that of the associated carbon atoms, and participated in the calculation of final *R* indices. All calculations were performed using the teXsan crystallographic software.[23]

General Procedure for Catalytic Study: In a typical reaction, the catalyst (0.003 mmol) in solvent (acetone, 3 mL) was placed in a 25 mL Schlenk tube and stirred for 10 min at 298 K in an argon atmosphere. The respective substrates (3 mmol) and chlorobenzene (GC internal standard) were added into the catalyst solution whilst stirring conditions. The oxidant (0.3 mmol H_2O_2) was added over a period of 20 h through a syringe pump.

$[Fe(PY_5Me_2)(CH_3CN)](ClO_4)_2$ (1): Equimolar amounts of PY_5Me_2 (88.6 mg, 0.2 mmol) and $Fe(ClO_4)_2{\cdot}6H_2O$ (72.6 mg, 0.2 mmol) were dissolved in CH_3CN (15 mL) and the solution was stirred at room temperature for 2 h in a nitrogen atmosphere. Addition of diethyl ether into the solution resulted in the precipitation of a yellow solid, which was collected by filtration. The compound was further purified by slow diffusion of diethyl ether into a CH_3CN solution of **1**. Yield: 90% (133.1 mg). **ESI/MS** (+ve mode): *m*/*z* 249.6 $[M - CH_3CN]^{2+}$; 598.2 $[M + ClO_4 - CH_3CN]^+$. **IR** (selected bands, KBr): $\tilde{\nu}$ = 2007 w, 1597 m, 1467 m, 1440 m, 1413 w, 1392 w, 1090 s, 864 w, 763 m, 623 m cm^{-1}. $C_{31}H_{28}Cl_2FeN_6O_8$: calcd. C 50.36; H 3.82; N 11.37%; found: C, 50.40; H, 3.90; N, 11.31%. **UV/Vis** (CH_3CN): λ_{max} [nm] (ε[$mol^{-1}dm^3cm^{-1}$]) 251 (21260), 353 (6703), 421 (7620).

$[Ni(PY_5Me_2)(CH_3CN)](ClO_4)_2$ (2): Equimolar amounts of PY_5Me_2 (88.6 mg, 0.2 mmol) and $Ni(ClO_4)_2{\cdot}6H_2O$ (73.1 mg, 0.2 mmol) were dissolved in CH_3CN (15 mL) and the solution was stirred at room temperature for 2 h. Addition of diethyl ether resulted in the precipitation of a green solid. The compound was further purified by slow diffusion of diethyl ether into a CH_3CN solution of **2**. Yield: 78% (115.8 mg). **ESI/MS** (+ mode): *m*/*z* 250.8 $[M - CH_3CN]^{2+}$; 600.4 $[M + ClO_4–CH_3CN]^+$. **IR** (selected bands, KBr): $\tilde{\nu}$ = 2018 w, 1596 m, 1465 m, 1454 m, 1440 m, 1389 w, 1299 w, 1108 s, 865 w, 764 m, 628 s cm^{-1}. $C_{31}H_{28}Cl_2N_6NiO_8$: calcd. C 50.17; H 3.80; N 11.32%; found: C 50.20; H 3.78; N 11.20%. **UV/Vis** (CH_3CN): λ_{max} [nm] (ε[$mol^{-1}dm^3cm^{-1}$]) 261 (17000), 309 (940).

Crystallographic data (excluding structure factors) for the structure in this paper have been deposited with the Cambridge Crystallographic Data Centre, CCDC, 12 Union Road, Cambridge CB21EZ, UK. Copies of the data can be obtained free of charge on quoting the depository number CCDC-930612 (**2**) (Fax: +44-1223-336-033; E-Mail: deposit @ccdc.cam.ac.uk, http://www.ccdc.cam.ac.uk).

Supporting Information (see footnote on the first page of this article): Selected bond parameters /Å,° for compound **2** (Table S1); Oxidation of cyclohexanol with H_2O_2 with **1** in various solvent (Table S2); A summary of crystal data, data collection, and structure refinement for **2** (Table S3). ESI-MS (+ ve mode) of **1** in CH_3CN [inset shows the expanded (top) and calculated (bottom) isotopic pattern of the peak at *m*/*z* at 598.2] (Figure S1). ESI-MS (+ ve mode) of **2** in CH_3CN [inset shows the expanded (top) and calculated (bottom) isotopic pattern of the peak at *m*/*z* at 600.6] (Figure S2).

Acknowledgements

The authors gratefully acknowledge the financial support of National Natural Science Foundation of China (21201023) and the Scientific Research Fund of HuBei Provincial Education Department (D20131202).

References

[1] a) A. J. Canty, N. J. Minchin, B. W. Skelton, A. H. White, *J. Chem. Soc. Dalton Trans.* **1986**, 2205; b) T. J. Morin, S. Wanniarachchi, C. Gwengo, V. Makura, H. M. Tatlock, S. V. Lindeman, B. Bennett, G. J. Long, F. Grandjeand, J. R. Gardinier, *Dalton Trans.* **2011**, *40*, 8024.

[2] R. J. M. Klein Gebbink, R. T. Jonas, C. R. Goldsmith, T. D. P. Stack, *Inorg. Chem.* **2002**, *41*, 4633.

[3] J. S. Huang, J. Xie, S. C. F. Kui, G. S. Fang, N. Y. Zhu, C. M. Che, *Inorg. Chem.* **2008**, *47*, 5727.

[4] C. R. Goldsmith, R. T. Jonas, A. P. Cole, T. D. P. Stack, *Inorg. Chem.* **2002**, *41*, 4642.

[5] D. E. Freedman, D. M. Jenkinsz, J. R. Long, *Chem. Commun.* **2009**, 4829.

[6] J. M. Zadrozny, D. E. Freedman, D. M. Jenkins, T. David Harris, A. T. Iavarone, C. Mathonière, R. Clérac, J. R. Long, *Inorg. Chem.* **2010**, *49*, 8886.

[7] D. E. Freedman, D. M. Jenkins, A. T. Iavarone, J. R. Long, *J. Am. Chem. Soc.* **2008**, *130*, 2884.

[8] B. Bechlars, D. M. D'Alessandro, D. M. Jenkins, A. T. Iavarone, S. D. Glover, C. P. Kubiak, J. R. Long, *Nat. Chem.* **2010**, *2*, 362.

[9] Y. Q. Zhang, C. L. Luo, *Polyhedron* **2011**, *30*, 3228.

[10] Y. J. Sun, J. P. Bigi, N. A. Piro, M. L. Tang, J. R. Long, C. J. Chang, *J. Am. Chem. Soc.* **2011**, *133*, 9212.

[11] H. I. Karunadasa1, C. J. Chang, J. R. Long, *Nature* **2010**, *464*, 1329.

[12] E. L. M. Wong, G. S. Fang, C. M. Che, N. Y. Zhu, *Chem. Commun.* **2005**, 4578.

[13] C. R. Goldsmith, A. P. Cole, T. D. P. Stack, *J. Am. Chem. Soc.* **2005**, *127*, 9904.

[14] R. T. Jonas, T. D. P. Stack, *J. Am. Chem. Soc.* **1997**, *119*, 8566.

[15] C. R. Goldsmith, R. T. Jonas, T. D. P. Stack, *J. Am. Chem. Soc.* **2002**, *124*, 83.

[16] See for example: a) I. Prat, A. Company, T. Corona, T. Parella, X. Ribas, M. Costas, *Inorg. Chem.* **2013**, *52*, 9229; b) A. Thibon, V. Jollet, C. Ribal, K. Senechal-David, L. Billon, A. B. Sorokin, F. Banse, *Chem. Eur. J.* **2012**, *18*, 2715; c) K. Moller, G. Wienhofer, K. Schroder, B. Join, K. Junge, M. Beller, *Chem. Eur. J.* **2010**, *16*, 10300; d) B. Wang, S. F. Wang, C. G. Xia, W. Sun, *Chem. Eur. J.* **2012**, *18*, 7332; e) E. A. Mikhalyova, O. V. Makhlynets, T. D. Palluccio, A. S. Filatov, E. V. Rybak-Akimova, *Chem. Commun.* **2012**, *48*, 687; f) Y. Hitomi, K. Arakawa, T. Funabiki, M. Kodera, *Angew. Chem. Int. Ed.* **2012**, *51*, 3448; g) M. Costas, L. Que, *Angew. Chem. Int. Ed.* **2002**, *41*, 2179.

[17] J. M. Smith, J. R. Long, *Inorg. Chem.* **2010**, *49*, 11223.

[18] T. J. Meyer, M. H. V. Huynh, *Inorg. Chem.* **2003**, *42*, 8140.

[19] W. W. Y. Lam, W. L. Man, T. C. Lau, *Coord. Chem. Rev.* **2007**, *251*, 2238.

[20] E. Alper Ünal, D. Wiedemann, J. Seiffert, J. P. Boyd, A. Grohmann, *Tetrahedron Lett.* **2012**, *53*, 54.

[21] A. Altomare, G. Cascarano, C. Giacovazzo, A. Guagliardi, M. Burla, G. Polidori, M. J. Camalli, *Appl. Crystallogr.* **1994**, *27*, 435.

[22] *DIRDIF 99*, P. T. Beurskens, G. Admiraal, G. Beurskens, W. P. Bosman, R. de Gelder, R. Israel, J. M. M. Smits, *The DIRDIF-99 Program System*; Technical Report of the Crystallography Laboratory, University of Nijmegen, The Netherlands, **1999**.

[23] *Crystal Structure*, Single Crystal Structure Analysis Software, Version 3.5.1; Rigaku/MSC Corporation: The Woodlands, TX, USA, Rigaku, Akishima, Tokyo, Japan, **2003**; D. J. Watkin, C. K. Prout, J. R. Carruthers, P. W. Betteridge, *Crystals*, Chemical Crystallography Lab, Oxford, UK, **1996**; issue 10.

Received: September 13, 2013
Published Online: February 4, 2014

